Materials Science-Poland, *Vol. 27*, *No. 3*, *2009*

Fabrication of mesoporous mixed oxides containing copper and cerium by using substituted anionic clays as precursors

G. CARJA*, S. DRANCA, G. CIOBANU, E. HUSANU, I. BALASANIAN

Faculty of Chemical Engineering and Environmental Protection,
Technical University "Gh. Asachi" of Iasi, Iasi 700554, Romania

Copper and cerium partially substituted anionic clay was synthesized by the coprecipitation method. The XRD analysis and N_2 adsorption at 77 K indicated that calcination destroys the layered matrix of the clay, giving rise to mixed oxides having a high surface area and mesoporous characteristics; SEM analysis showed that the new formed mixed oxides consist of ensembles of highly agglomerated, interconnected nanoparticles. It results from XPS that copper and cerium both contribute to establish the specific redox properties on the surface.

Key words: *copper; cerium; mixed oxides; mesoporosity; textural characteristics*

1. Introduction

Nowadays, continuous efforts have been made to develop new and superior catalytic systems for removing toxic environmental pollutants, CO being one of the most dangerous of such pollutants. A selective oxidation seems to be the simplest way to remove it [1]. Recently, reported results show that a cost effective and promising catalytic system for the selective oxidation of CO is based on copper–cerium mixed oxides [2]. Not only the composition but also textural and surface properties are important to establish the catalytic performance of mixed oxides containing copper and cerium; the specific ensembles of the catalyst nanoparticles, more precisely their shape, size and the configuration pattern giving rise to tailored nanoporous properties and high surface areas are important for the practical applications of these materials [3]. Represented by a general formula $[M^{II}_{1-x}M^{III}_{x}(OH)_2]^{x+}$ $[A^{m-}_{x/m} \cdot nH_2O]^{x-}$, layered double hydroxides anionic clays (LDHs) are built up of sheets of edge sharing metal octahedra, where in

*Corresponding author, e-mail: carja@uaic.ro

comparison with brucite $M(OH)_2$, part of the M^{II} is replaced by M^{III} metal cations; the excess positive charge is counterbalanced by exchangeable anions A^{m-}, located as water molecules, in the interlayer space [4]. The large variety of compositions that can be developed by altering the nature of the divalent and trivalent cations (M^{II}, M^{III}), the interlayer anions (A^{m-}) and the stoichiometric coefficient (x), give rise to a large diversity of layered, anionic, clay like structures, [5]. The thermal decomposition of hydrotalcite-like materials around 773 K gives rise to stable homogeneous and highly dispersed mixed metal oxides with a high surface area and specific acid–base/redox and textural properties with well known applications as catalysts [6–8]. Based on this data, we have synthesized copper and cerium partially substituted hydrotalcite-like anionic clays and further used them as precursors to obtain, for the first time to our knowledge, copper and cerium containing mixed oxides of specific mesoporous properties. We also present here the textural and surface properties of the new material.

2. Experimental

Sample syntheses. The hydrotalcite like samples were synthesized by the coprecipitation method in low saturation conditions [9], at 313 K, under a bubbling, constant flow of nitrogen and under vigorous stirring.

CuCeLDH: the precipitants NaOH, Na_2CO_3 and metal salts used as precursors: $Mg(NO_3)_2{\cdot}6H_2O$ (0.015 mol), $Al(NO_3)_3{\cdot}9H_2O$ (0.005 mol), $Cu(NO_3)_2{\cdot}3H_2O$ (0.015 mol), $CeNO_3{\cdot}\ 6H_2O$ (0.005 mol) were added dropwise together in such a way that the pH of the synthesis medium was kept at a constant level of 8.9 ± 0.2. The resulting light blue precipitate was aged at 305 K for 8 h under mild stirring, separated by centrifugation, washed extensively with warm, deionized water until sodium free, and dried under vacuum at 338 K. The CuCeLDH sample was calcined in air at 723 K (the temperature was raised at 8 $K{\cdot}min^{-1}$ to 723 K, maintained there for 7 h and then cooled slowly in nitrogen) is denoted as cCuCeLDH.

MgAlLDH: 100 cm^3 of aqueous solution of $Mg(NO_3)_2{\cdot}6H_2O$ (0.03 mol), $Al(NO_3)_3{\cdot}9H_2O$ (0.01 mol) and aqueous solution of the precipitants NaOH, Na_2CO_3 were added dropwise together in such a way that the pH remained constant (pH = 9.5). The resulting white precipitate was aged at 338 K for 24 h under stirring, separated by centrifugation, washed extensively with warm deionized water until sodium free and then dried under vacuum at 338 K.

Characterization. The chemical compositions of the synthesized samples were determined by X-ray fluorescence spectroscopy (Rigaku RIX2000 sequential X-ray fluorescence spectrometer).

XRD: X-ray powder diffraction patterns were recorded with a Philips PW 1840 diffractometer using monochromatic CuK_α radiation ($\lambda = 0.154$ nm), operating at 40 kV and 30 mA over a 2θ range from 4 to 70 degree. N_2 adsorption isotherms were measured on a Coulter SA 3100 automated gas adsorption system. Prior to the measurements,

the samples were heated under vacuum at 383 K for 5 h in order to expel the interlayer water molecules. Microcomputer processing controlled the analysis. The BET specific surface area (S_{BET}) was calculated by the standard Brunauer, Emmett and Teller method based on adsorption data [10]. Pore size distributions were calculated from the desorption branches of the isotherms by the Barret, Joyner and Halenda method [11] and the corrected Kelvin equation. Pore volume (V_p) values were determined by the De Boer t-plot method [12]. X-ray photoelectron spectra (XPS) were recorded using a Perkin Elmer model 5500-MT (ESCA/MC/SAM) surface science instrument equipped with a magnesium anode (1253.6 eV) operating at 15 kV and 20 mA. A microcomputer processor controlled the spectra acquisition and data handling. Samples were analyzed as powders dusted onto a double sided sticky tape in an analysis chamber, typically operating at 10^{-9} Torr. All binding energy values were determined with respect to the C 1s line (284.6 eV) of the carbon overlayer, and the standard deviation of the peak position was within ± 0.1 eV. The surface (XPS) concentration of each element, expressed as surface atomic ratios, was calculated from the corresponding peak areas using specific atomic sensitivity factors, with the integral subtraction of the background noise [13]. A Hitachi S-800 scanning electron microscope was utilized for scanning electron microscopy (SEM).

3. Results and discussion

The results of chemical analyses of the samples are given in Table 1; the experimental XRD results are coincident, within experimental errors, with those of the starting mixed aqueous solutions.

Table 1. Chemical compositions, lattice parameters and porosity characteristics of the studied samples

Sample	Lattice parameters [Å]		Molar fraction				S_{BET} [m^2/g]	C_{BET}	V_p [cm^3/g]	% µpA
	a	*c*	Mg	Cu	Ce	Al				
MgAlLDH	3.059	23.37	0.74	–	–	0.25	94.5	27.9	0.431	-
CuCeLDH	3.067	22.79	0.37	0.34	0.14	0.15	69.3	16.7	0.177	-
cCuCeLH	-	-	0.34	0.35	0.17	0.14	134.4	401.9	0.381	14

Figure 1 shows the powder XRD patterns of the as-synthesized and also thermally treated (723 K and 1173 K) copper and cerium containing layered double hydroxides. For CuCeLDH, the diffraction peaks are typical of a double layered hydroxidestructure [4] with sharp and symmetric reflections of the basal (003), (006), and (009) planes and broad, less intense, asymmetric reflections for the nonbasal (012), (015) and (018) planes; the XRD reflections were indexed using a hexagonal cell with a rhombohedral symmetry ($R\bar{3}m$), commonly used as a description of the LDH structure. The parameter *a*, calculated as 2*d*(110), is a function of the metal–metal distance within the layers, pointing out the cations stacking in (003) planes, while the *c* parame-

ter, calculated as 3*d*(003), is a function of the average charge of the metal cations, the nature of the interlayer anions and the water content of the hydrotalcite like sample.

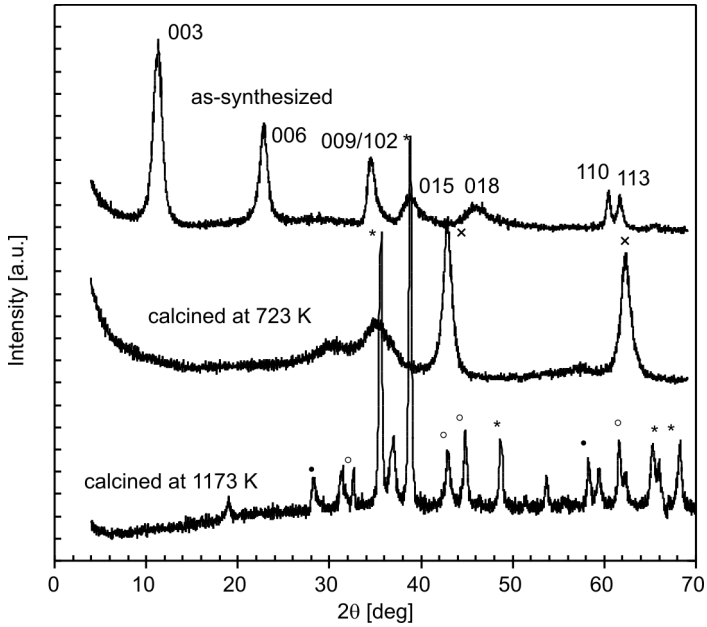

Fig. 1. The XRD patterns of CuCeLDH: ∗ _ cooper oxide, ● – cerium oxide, ○ – $MgAl_2O_4$ spinel like phase, × – MgO

The XRD parameters are shown in Table 1. The value of the lattice parameter *a* is equal to 3.059 Å for MgAlLDH, but the corresponding value increases to 3.067 Å for CuCeLDH. The increase in the parameter *a* for CoCeLDH indicates that Ce^{3+} ions replace Al^{3+} ions in the brucite-like layers, and that is because the ionic radius of Ce^{3+} (Shannon ionic radius 1.01 Å [14]) is larger than the ionic radius of Al^{3+} (Shannon ionic radius 0.53 Å), while a correspondence exists between the ionic radius of Cu^{2+} hexacoordinate (Shannon ionic radius 0.73 Å) and the ionic radius of Mg^{2+} hexacoordinate (Shannon ionic radius 0.72 Å). The decrease in the *c* parameter can be attributed to the modified electrostatic interactions between the layer and the interlayer network when copper and cerium ions are introduced in the LDH layer. After calcination at 723 K, the hydrotalcite structure completely collapses and the new reflections indicate the presence of poorly crystallized mixed oxides, characteristic of the LDHs calcined at this temperature [1, 3]. The XRD pattern of the samples, calcined at 1173 K for 8 h, gives information about the evolution of the newly formed mixed oxides; the corresponding XRD pattern (see Fig. 1) shows strong peaks characteristic of a well defined phase of CuO (JCPDS file 5-0661) and also low intensity peaks characteristic of the CeO_2 phase [15].

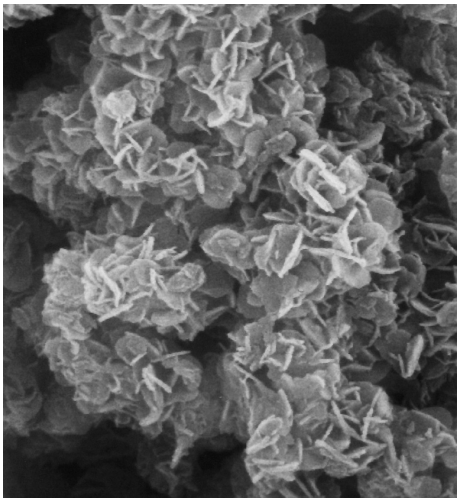

Fig. 2. The SEM image of cCuCeLDH

The SEM image of the cCuCeLDH is presented in Fig. 2. It indicates a high crystalline material formed by enough uniform and highly interconnected particles with an average diameter equal to 110 nm. The nitrogen adsorption isotherms of CuCeLDH and cCuCeLDH are shown in Fig. 3. Their different appearances suggest differences in the porosity characteristics after thermal treatment. For the CuCeLDH a type IV isotherm with a type H_3 hysteresis loop and no limiting adsorption at p/p_0 values close to unity is obtained. The broadness of the hysteresis loop reveals highly non-uniform pore-size and/or shape. This result indicates that Cu and Ce containing LDH consists of aggregates of plates or edged particles forming slit shaped pores, which are characteristics of LDH like materials.

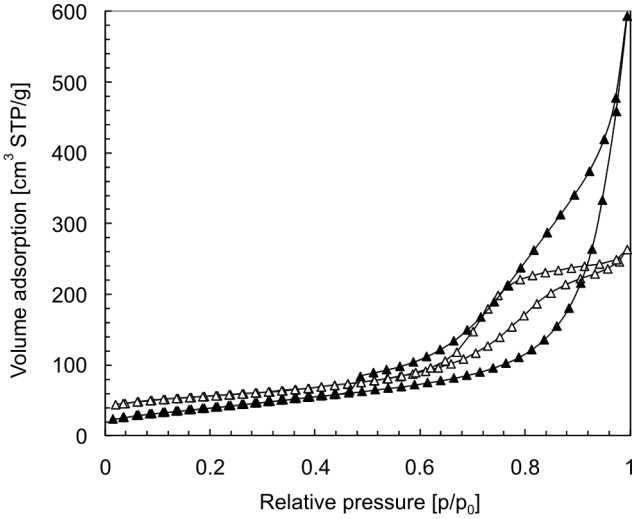

Fig. 3. N_2 adsorption–desorption isotherms of:
▲ – CuCeLDH and Δ – cCuCeLDH

For cCuCeLDH, the multilayer adsorption at p/p_0 values close to zero, as well as for a high value of the *C* constant in the BET equation (see Table 1) indicate that some microporosity features developed in the sample [16]; furthermore, a much lower adsorption value at p/p_0 close to unity shows that larger mesopores and macropores are absent in this sample. In general, in the LDHs, mesopore formation is through interparticle packing, while the distribution of pores is influenced by the crystallite size and packing arrangement of crystallites [17, 18]. In the case of the mixed oxides, obtained after subjecting the LDHs to thermal treatment at 723 K, the loss of interlayer water and interlayer anions (e.g., CO_3^{2-}, NO_3^-) by a cratering mechanism during calcination [9] allows the formation of micropores and gives rise to an important increase in the surface area and pore volume, as results from Table 1.

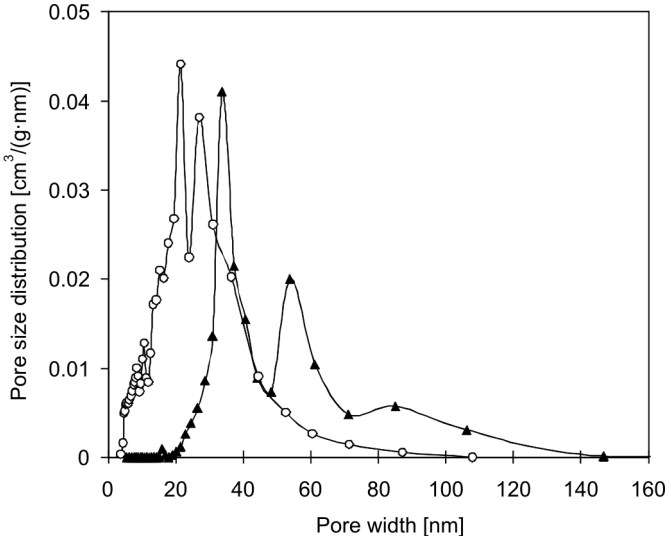

Fig. 4. Pore size distributions of: ▲ – CuCeLDH and ∘ – cCuCeLDH

Pore size distribution (PSD) is further used to study the sample porosity. The PSD curves presented in Fig. 4 also indicate the change in the porous features of CuCeLDH after thermal treatment. The PSD curve of CuCeLDH is defined by two maxima at 34 and 57 nm. For cCuCeLDH, the PSD curve is shifted to the left with two maxima at 21 and 27 nm, thus indicating clearly the decrease in the pore sizes after the thermal treatment. This behaviour is characteristic of hydrotalcite like materials [17, 18]. The data of Table 1 reveal that the S_{BET} value of MgAlLDH reaches 94.5 m^2/g, though the corresponding value for CuCeLDH is equal to 69.3 m^2/g. Calcination gives rise to a slight increase in the S_{BET} value, to 134.4 m^2/g, for cCuCeLDH, though the corresponding value of the calcined MgAlLDH reaches 167 m^2/g. Pore volume (V_p) decreases after Cu and Ce were introduced in the layered clay, reaching 0.381 cm^3/g for cCuCeLDH, in comparison with 0.483 cm^3/g for the calcined MgAlLDH.

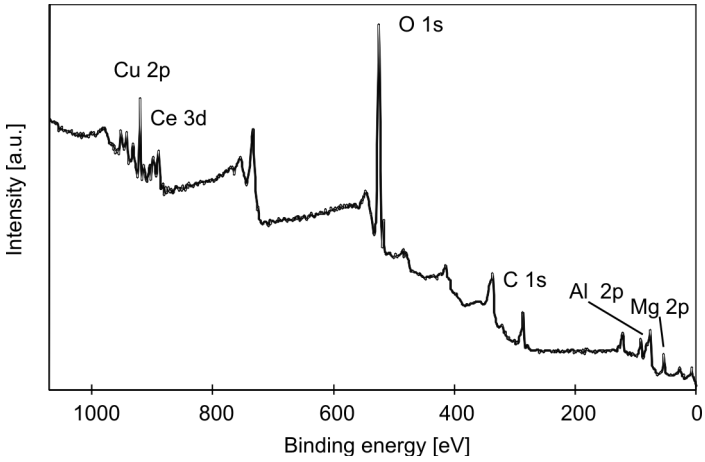

Fig. 5. XPS pattern of cCuCeLDH

The nature of the active species present on the surface is important for establishing the properties of the catalytic samples. Taking this into account, XPS analysis was performed in order to obtain information about the surface composition of the Cu–Ce mixed oxides derived from copper and cerium substituted hydrotalcite-like samples.

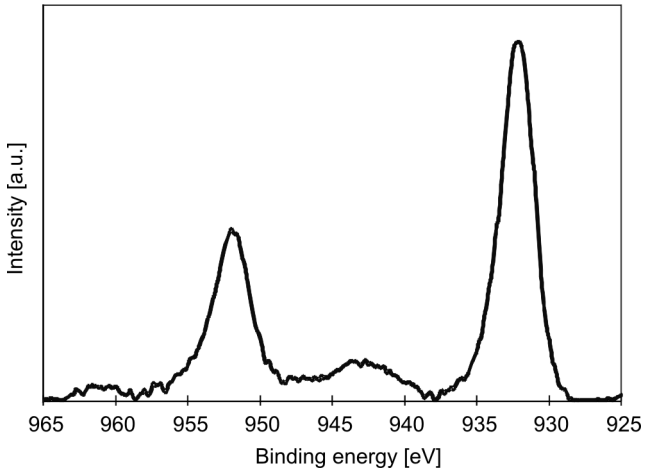

Fig. 6. Cu 2p XPS spectra in cCuCeLDH sample

The corresponding XPS pattern of cCuCeLDH, presented in Fig. 5, shows that all the elements are present on the sample surface. A closer look at the Cu 2p XPS spectra (Fig. 6) reveals the presence of shake-up satellite features for both Cu 2p3/2 and Cu 2p1/2, thus indicating that Cu^{2+} ions [19] are present on the surface of cCuCeLDH. The pattern characteristic of the Ce 3d XPS spectra (Fig. 7) suggests that a redox couple $Ce^{4+/}Ce^{3+}$ [20, 21] is present on the sample surface; the state of the surface copper

together with the different contribution of the surface Ce^{4+} and Ce^{3+} point to specific surface features of mixed oxides obtained from LDH containing copper and cerium.

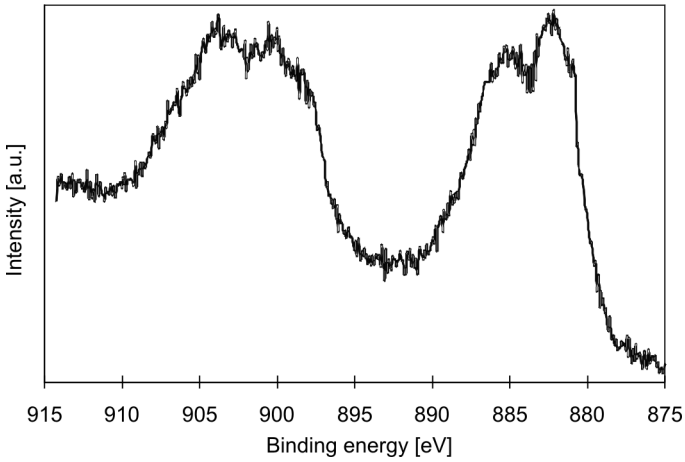

Fig. 7. Ce 3d XPS spectra in cCuCeLDH sample

4. Conclusions

Copper and cerium substituted layered double hydroxides were used as precursors for obtaining mixed oxides with specific textural and surface properties. XRD analysis demonstrates the formation and evolution of an LDH layered structure, after the thermal treatment, to the mesoporous mixed oxides. The SEM image shows the formation of overlapped, highly agglomerated nanoparticles, irregular in size and/or shape and with an average diameter equal to 110 nm. The presence of Cu^{2+} and the redox couple $Ce^{4+/}Ce^{3+}$ on the surface contribute to design-specific surface properties for the newly formed mixed oxides. Further works aim to test this material as a catalyst in CO selective oxidation.

Acknowledgement

This research was partially supported by the PNCDI II contracts NATOEPA 71-020/2007 and LACAFIA 134 CPI/2007.

References

[1] AVGOUROPOULOS G., IOANNIDES T., Appl. Catal., B, 67 (2006), 11.
[2] ZHENG X.C., WANG S.P., WANG S.R., ZHANG S.M., HUANG W.P., WU S.H., Mater. Sci. Eng., C, 25 (2005), 516.
[3] RIVES V., *Layered Double Hydroxides: Present and Future*, Nova Sci. Pub. Inc., New York, 2001.
[4] CAVANI F., TRIFIRO F., VACCARI A., Catal. Today, 11 (1991), 173, and references therein.
[5] ARCO M., GUTIERREZ S., MARTIN C., RIVES V., ROCHA J., J. Solid State Chem., 177 (2004), 3954.

[6] VACCARI A., Appl. Clay Sci., 14 (1999), 161.
[7] CARJA G., NAKAMURA R., AIDA T., NIIYAMA H., J. Catal., 218 (2003), 104.
[8] KANNAN S., DUBEY A., KNOZINGER H., J. Catal., 2312 (2005), 381.
[9] REICHLE W.T., YANG S.Y., EVERHARDT S.D., J. Catal., 10 (1986), 352.
[10] BRUNAUER S., EMMETT P.H., TELLER E., J. Am. Chem. Soc., 60 (1938), 309.
[11] SING K.S.W., EVERETT D.H., HAUL R.A.W., MOSCOU L., PIEROTTI R.A., ROUQUEROL J., SIEMIENIEWSKA T., Pure Appl. Chem., 57 (1985), 603.
[12] GREGG S.J., SING K.S.W., *Adsorption, Surface Area and Poros*ity, 2nd Ed., Academic Press, London, 1982.
[13] DEFFOSE C., [in:] *Chemical Industries*, F. Dellany (Ed.), Marcel Dekker, New York, 1984, p. 225.
[14] SHANNON R.D., Acta Crystallogr., Sect. A: Found. Crystallogr., 32 (1976), 751.
[15] MOGENSENA M., SAMMES N.M., TOMPSETT G.A., Solid State Ionics, 129 (2000), 63.
[16] ZARĘBA-GRODŹ I., MIŚTA W., SIKORA A., GOTSZALK T., STRĘK W., HERMANOWICZ K., MARUSZEWSKI K., Mater. Sci., 23 (2005), 147.
[17] HUTSON N.D., Chem. Mater., 16 (2004), 4135.
[18] TAKEHIRA K., KAWABATA T., SHISHIDO T., MURAKAMI K., OHI T., SHORO D., HONDA M., TAKAKI K., J. Catal., 231 (2005), 92.
[19] CARJA G., NAKAMURA R., NIIYAMA H., Microporous Mesoporous Mater., 83 (2005), 147.
[20] WAGNER C.D., RIGGS W.N., DAVIS L.E., MOULDER J.F., MUILENBERG G.E., *Handbook of X-Ray Photoelectron Spectrometry*, Perkin-Elmer, Eden Praine, 1979.
[21] LAACHIR A., PERRICHON V., BADRI A., LAMOTTE J., CATHERINE E., LAVALLEY J.C., FALLAH J., HILAIRE L., NORMAND F., QUEMERE E., SAUVION G.N., TOURET O.J., J. Chem. Soc., Faraday Trans., 87 (1991), 1601.
[22] GROEN J.C., PEFFER L.A.A., PEREZ-RAMIREZ J., Microporous Mesoporous Mater., 60 (2003), 1.

Received 2 October 2008
Revised 19 January 2009